ACS central science

Research Article

Cite This: ACS Cent. Sci. 2019, 5, 1929−1936

http://pubs.acs.org/journal/acscii

Micrococcal-Nuclease-Triggered On-Demand Release of Vancomycin from Intramedullary Implant Coating Eradicates *Staphylococcus aureus* Infection in Mouse Femoral Canals

Ananta Ghimire, Jordan D. Skelly, and Jie Song*

Department of Orthopedics and Physical Rehabilitation, University of Massachusetts Medical School, Worcester, Massachusetts 01655, United States

Supporting Information

ABSTRACT: Preventing orthopedic implant-associated bacterial infections remains a critical challenge. Current practices of physically blending high-dose antibiotics with bone cements is known for cytotoxicity while covalently tethering antibiotics to implant surfaces is ineffective in eradicating bacteria from the periprosthetic tissue environment due to the short-range bactericidal actions, which are limited to the implant surface. Here, we covalently functionalize poly(ethylene glycol) dimethacrylate hydrogel coatings with vancomycin via an oligonucleotide linker sensitive to *Staphylococcus aureus* (*S. aureus*) micrococcal nuclease (MN) (PEGDMA-Oligo-Vanco). This design enables the timely release of vancomycin in the presence of *S. aureus* to kill the bacteria both on the implant surface and within the periprosthetic tissue environment. Ti6Al4V intramedullary (IM) pins surface-tethered with dopamine methacrylamide (DopaMA) and uniformly coated with PEGDMA-Oligo-Vanco effectively prevented periprosthetic infections in mouse femoral canals inoculated with bioluminescent *S. aureus*. Longitudinal bioluminescence monitoring, μCT quantification of femoral bone changes, end point quantification of implant surface bacteria, and histological detection of *S. aureus* in the periprosthetic tissue environment confirmed rapid and sustained bacterial clearance by the PEGDMA-Oligo-Vanco coating. The observed eradication of bacteria was in stark contrast with the significant bacterial colonization on implants and osteomyelitis development found in the absence of the MN-sensitive bactericidal coating. The effective vancomycin tethering dose presented in this on-demand release strategy was >200 times lower than the typical prophylactic antibiotic contents used in bone cements and may be applied to medical implants and bone/dental cements to prevent periprosthetic infections in high-risk clinical scenarios. This study also supports the timely bactericidal action by MN-triggered release of antibiotics as an effective prophylactic method to bypass the notoriously harder to treat periprosthetic biofilms and osteomyelitis.

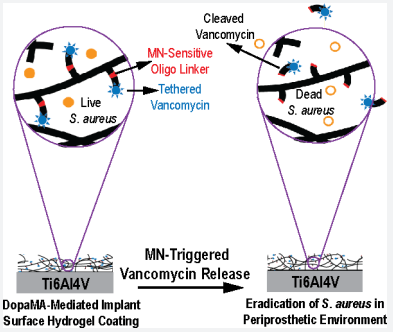

INTRODUCTION

Periprosthetic infections represent occasional but serious health threats. Bacterial colonization around implants and subsequent biofilm formation are difficult to treat and could lead to implant failure, requiring major revision surgeries associated with high treatment cost, high morbidity, and even mortality.[1−3] There are no effective strategies for eradicating established biofilms or bacteria harboring within dense tissues such as the canaliculi of bone due to poor penetration of antibiotics and immune cells into the dense matrices of biofilm and cortical bone.[4−7] Thus, prophylactic strategies, particularly in high-risk patient populations and/or following high-risk clinical procedures, that ensure timely elimination of bacteria within the implant microenvironment thereby preventing biofilm formation or bacteria invasion into bone canaliculi would be highly desired.

A current clinical practice for preventing infections in high-risk orthopedic joint replacement surgeries involves physical blending of antibiotics with bone cements. This approach, however, requires high antibiotic loading that could exert local and systemic cytotoxicity. Delivering antibiotics via non-covalent implant surface coatings has been pursued as a safer alternative,[8,9] although achieving suitable antibiotic release kinetics to ensure adequate and prompt release remains a challenge.[8,10−15] Antibiotics covalently attached to implant surfaces[4,16,17] have also been shown to exert bactericidal properties when they are presented via linkers or polymer chains of suitable flexibility/lengths[18,19] at a modification site minimally perturbing the bioactivity of the drug.[20] A limitation of this covalent surface modification approach, however, is that the antibiotic action is restricted to the immediate surface of the implant. For instance, we recently demonstrated that vancomycin covalently conjugated to the polymer brushes grafted from Ti6Al4V intramedullary (IM) pins was able to significantly reduce the colonization/growth of *Staphylococcus aureus* (*S. aureus*) on the metallic implant surface.[21] Complete eradication of bacteria within the periprosthetic IM tissue environment, however, was not achieved due to the inability of the covalently tethered vancomycin to diffuse away from the Ti6Al4V surface.

Received: August 27, 2019
Published: December 10, 2019

DOI: 10.1021/acscentsci.9b00870
ACS Cent. Sci. 2019, 5, 1929−1936

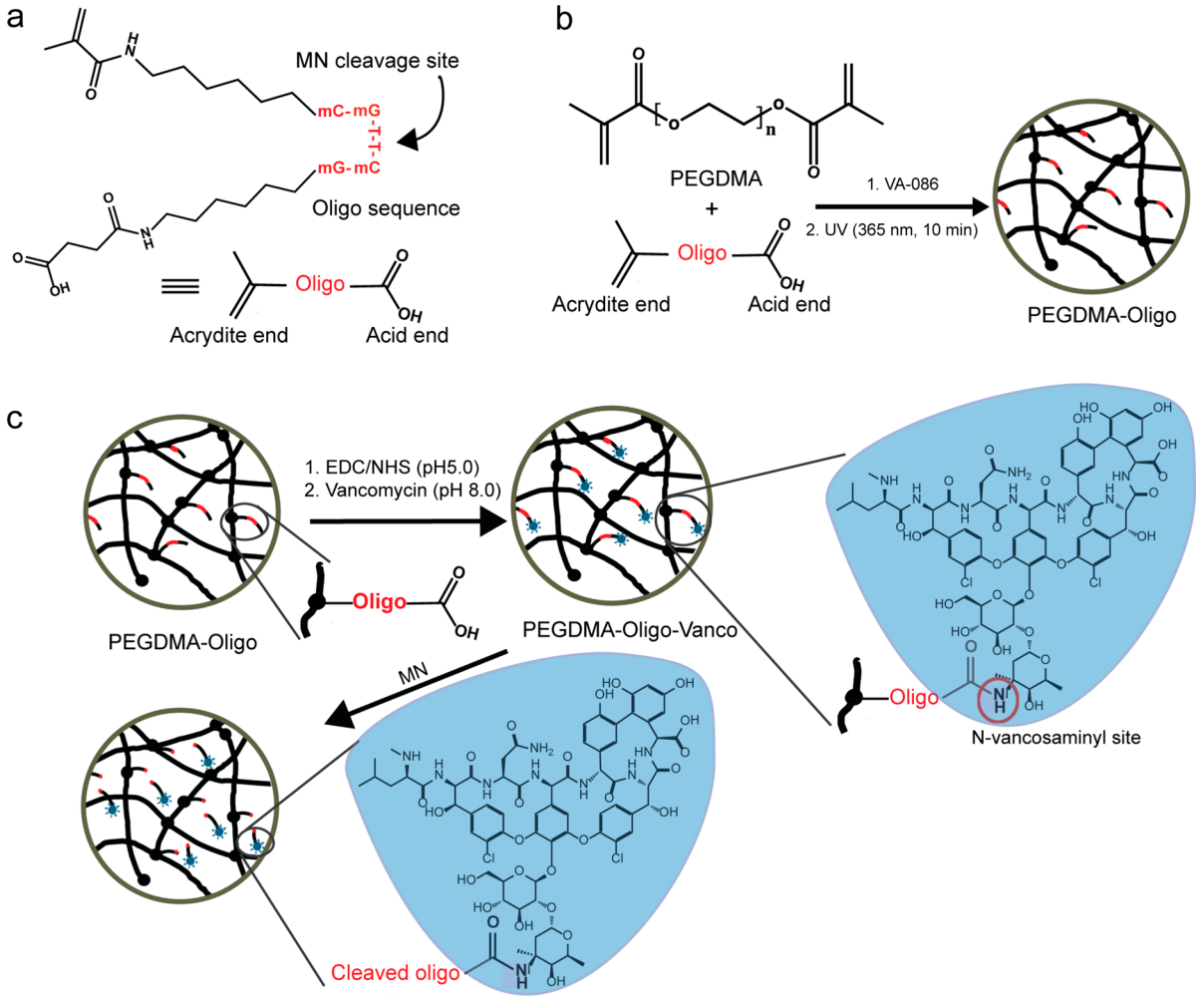

Figure 1. Depiction of the PEGDMA-Oligo-Vanco hydrogel network and MN-triggered vancomycin release. (a) Oligonucleotide (Oligo) sequence modified with bifunctional end groups. (b) PEGDMA-Oligo hydrogel formation. (c) PEGDMA-Oligo-Vanco hydrogel formation and MN-triggered vancomycin release.

We envision that the covalent attachment of antibiotics to the implant surface via a linker sensitive to unique bacterial enzymatic activities could bridge the gap among the existing approaches. The timely on-demand release of free antibiotics from covalently modified implant surfaces could help combat infections within a broader periprosthetic tissue microenvironment while mitigating cytotoxicity associated with the burst release of high doses of physically entrapped antibiotics or risks for developing bacteria resistance due to inadequate/delayed antibiotic releases.[18,22] Various advanced drug delivery systems utilizing external stimuli such as pH, temperature, magnetic field, and ultrasound to trigger drug release were developed.[23−27] More recently, endogenous enzymatic activities (especially proteases and nucleases) have been exploited as more biologically relevant and safer alternatives to stimulate on-demand drug release from peptide- and nucleotide-based delivery systems.[23] Nonspecific cleavages of the peptide and oligonucleotide in these systems, however, present barriers to the success of this approach. Oligonucleotide sequences with 2′-*O*-carboxymethyl modifications were recently shown to improve cleavage specificity[27] by micrococcal nucleases (MNs) of *S. aureus*, the Gram-positive bacterium responsible for a third of all orthopedic implant related infections and a major cause of osteomyelitis.[3] The therapeutic efficacy of the MN-triggered release of physically entrapped vancomycin in silica nanocapsules was demonstrated *in vitro*.[28,29] However, *in vivo* efficacy of this approach, especially in the context of on-demand release of covalently tethered antibiotics for combating periprosthetic infections, is unknown.

Here, we covalently functionalize PEGDMA hydrogel with vancomycin via a 2′-*O*-carboxymethyl modified oligonucleotide linker sensitive to *S. aureus* MN and evaluate its antibacterial activity *in vitro* and antiperiprosthetic infection properties *in vivo* upon application to metallic implants as a surface coating using a rodent femoral canal infection model. The oligonucleotide linker (abbreviated as oligo, Figure 1a) consists of a carboxylic acid and an acrydite on either end of the mC−mG−T−T−mC−mG sequence, which was previously shown to exhibit enhanced stability to mouse and human serum but sensitivity to *S. aureus* MN cleavages.[28−30] The acrydite end is used to covalently conjugate the probe to the PEGDMA matrix during radical polymerization (Figure 1b) while the carboxylic acid end of the oligo linker is used to form an amide linkage with the *N*-vancosaminyl group of vancomycin via EDC/NHS chemistry (Figure 1c). Vancomycin, a glycopeptide antibiotic acting at the Gram-positive bacterial cell walls to block peptidoglycan synthesis, is considered the most effective in treating infections caused by

DOI: 10.1021/acscentsci.9b00870
ACS Cent. Sci. 2019, 5, 1929−1936

Staphylococcus including Methicillin-resistant *S. aureus*.[31] It inhibits the transpeptidation and transglycosylation steps of bacterial cell wall biosynthesis through the binding of the L-Lys−D-Ala−D-Ala termini of the nascent peptidoglycan precursor through H-bonds. Chemical modification at the *N*-vancosaminyl site is known to present minimal perturbation to this binding.[32,33] The flexible C5 spacers between the nucleotide sequence and the bifunctional end groups are designed to relieve steric hindrance during amidation with vancomycin via the *N*-vancosaminyl site and to ensure adequate rotational freedom of the oligo upon covalent attachment to the hydrogel matrix. In the presence of metabolically active *S. aureus*, the bacterial MN is expected to cleave the oligo at the unmodified T−T position, releasing the vancomycin with a small overhung fragment at the *N*-vancosaminyl site (Figure 1c). We recently showed that the minimal effective concentration of vancomycin (against *S. aureus*) was not significantly altered upon modification with an *N*-vancosaminyl oligo(ethylene glycol) overhang,[21] which is of comparable length of the amidated oligo fragment overhang upon MN cleavage.

RESULTS AND DISCUSSION

Synthesis of PEGDMA-Oligo and PEGDMA-Oligo-Vanco Hydrogels. We first validated the cleavage of the oligo probe (synthesized and purified by Integrated DNA Technologies) by MN (source: *S. aureus* strain ATCC 27735; Worthington Biochemical Corporation) prior to its conjugation with vancomycin or PEGDMA hydrogel. Gel permeation chromatography (GPC) and UV detection at 260 nm revealed two fragments upon treatment of the oligo by MN (0.1 U/μL) in PBS (pH 7.4, 10 mM) containing a physiological concentration of calcium ions (Figure 2a, blue trace). In the absence of calcium ions, MN showed very little cleavage of oligo (Figure 2a, red trace).

Upon confirmation of the sensitivity of the oligo to MN cleavage, it was covalently incorporated with PEGDMA during photopolymerization. A leaching experiment showed that 90 ± 5.0% oligo was effectively tethered to a 15 w/v% PEGDMA hydrogel, achieving 1.1 μg oligo/mg PEGDMA incorporation content, as revealed by the detection of untethered oligo (absorption at 260 nm) leached into deionized (DI) water upon extensive equilibration of the PEGDMA-Oligo hydrogel in PBS (48 h).

Covalent attachment of vancomycin to PEGDMA-Oligo hydrogel was carried out using EDC/NHS chemistry resulting in the PEGDMA-Oligo-Vanco hydrogel. To examine the release of covalently tethered vancomycin from the hydrogel, PEGDMA-Oligo-Vanco hydrogel discs (50 μL, 8 mm in diameter, n = 3) were incubated in PBS (pH 7.4, 10 mM) containing a physiological concentration of calcium ions with or without the presence of MN (0.1 and 1.0 U/μL). The concentration of released vancomycin was monitored by UV spectroscopy at 280 nm. As shown in Figure 2b, the release of vancomycin was only detected in the groups spiked with MN, supporting cleavage of the oligo linker and release of vancomycin by MN activity. The initial release (first 4 h) of vancomycin was slightly higher with the higher MN concentration, although the total vancomycin released over 24 h was the same. Assuming complete release of vancomycin after 24 h, the amount of vancomycin loaded on the 15 w/v% PEGDMA hydrogel matrix was 90 μg/mm^3 hydrogel (or 24 mg Vanco/40 g PEGDMA; note that the minimum inhibitory concentration of vancomycin was ~2 μg/mL[21]). This vancomycin covalent loading content was significantly lower than the noncovalent prophylactic antibiotics incorporation content in commercial bone cement (e.g., 0.5−1.0 g gentamycin/40 g bone cement, 1.0 g tobramycin/40 g bone cement).[34−37]

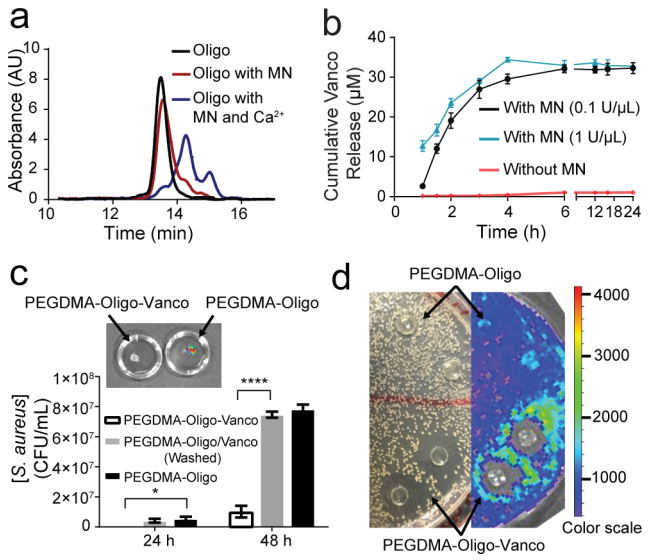

Figure 2. MN-triggered oligo cleavage and the antibacterial activities of PEGDMA-Oligo-Vanco hydrogel *in vitro*. (a) GPC traces of intact oligo (black) and oligo upon treatment with MN with (blue) and without (red) Ca^{2+}. (b) Cumulative vancomycin (Vanco) release from PEGDMA-Oligo-Vanco hydrogel incubated with (black and blue) and without (red) MN. Differences at all given time points were significant ($p \leq 0.0001$). (c) Total bacterial counts after 24 and 48 h of Xen-29 *S. aureus* culture in LB media containing PEGDMA-Oligo-Vanco, washed PEGDMA-Oligo/Vanco, or PEGDMA-Oligo hydrogels (n = 3; inset, corresponding IVIS image of the PEGDMA-Oligo-Vanco and PEGDMA-Oligo hydrogels retrieved after 48 h in *S. aureus* culture). (d) Photograph (left) and IVIS image (right) of an LB agar plate of Xen-29 *S. aureus* culture 24 h after placement of PEGDMA-Oligo-Vanco and PEGDMA-Oligo hydrogel discs (n = 2 shown) over the agar plate. Error bars represent standard deviations. * $p \leq 0.05$, ** $p \leq 0.01$, *** $p \leq 0.001$, **** $p \leq 0.0001$ (two-way ANOVA).

***In Vitro* Antibacterial Activity of PEGDMA-Oligo-Vanco Hydrogel.** The therapeutic efficacy of PEGDMA-Oligo-Vanco hydrogel was first evaluated by *in vitro* bacterial cultures. PEGDMA-Oligo-Vanco and PEGDMA-Oligo hydrogel discs (50 μL, 8 mm in diameter, n = 3) were incubated in Luria−Broth (LB) containing 130 CFU of *S. aureus* at 37 °C. To account for potential contribution from residue unconjugated vancomycin, another control group with the same content of vancomycin physically entrapped (without EDC/NHS) at the time of PEGDMA-Oligo hydrogel formation was also prepared (PEGDMA-Oligo/Vanco). All hydrogels were washed for 72 h in DI water before being placed in Xen-29 *S. aureus* suspension culture. The Xen29 *S. aureus*, emitting bioluminescence when metabolically active due to the expression of luciferase,[38] enables convenient visualization *in vitro* and longitudinal monitoring *in vivo* by an *in vivo* imaging system (IVIS-100, PerkinElmer). As shown in Figure 2c, the PEGDMA-Oligo-Vanco hydrogel was able to significantly inhibit the bacterial growth by 8-fold after 48 h. Of note, IVIS imaging showed no signs of bacterial attachment and colonization on the surface of the PEGDMA-Oligo-Vanco hydrogel upon its retrieval from the suspension culture after 48

DOI: 10.1021/acscentsci.9b00870
ACS Cent. Sci. 2019, 5, 1929−1936

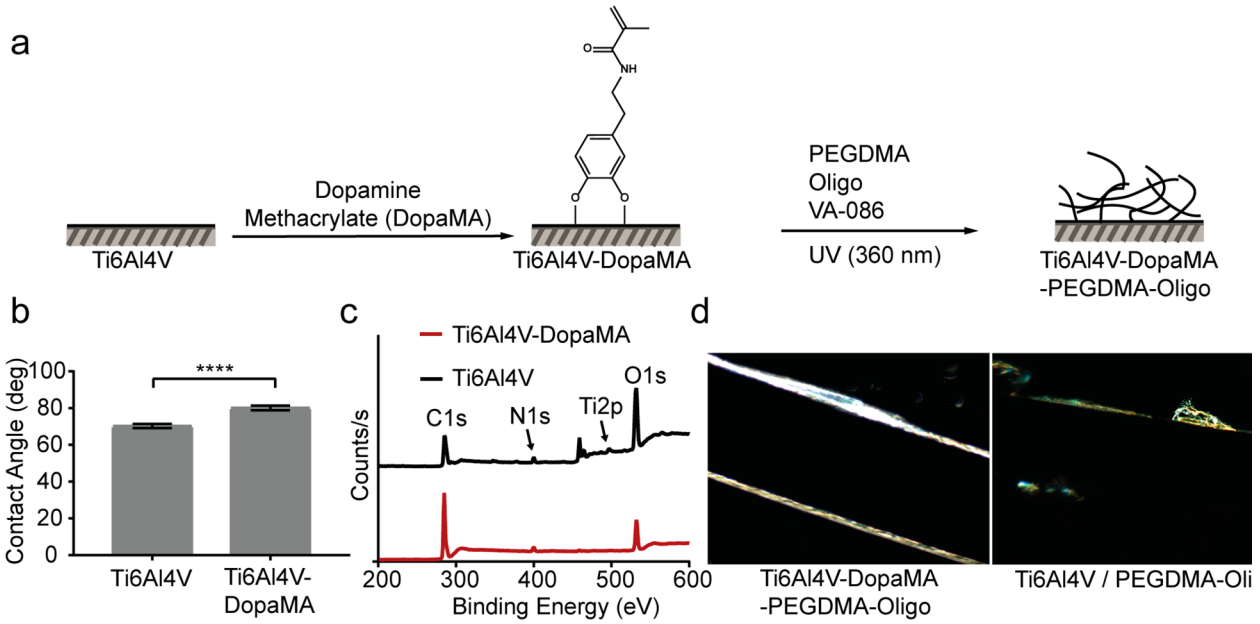

Figure 3. Surface modification and characterization of Ti6Al4V plates. (a) Schematic of sequential DopaMA and PEGDMA-Oligo hydrogel coatings on Ti6Al4V substrates. (b) Water contact angle ($n = 6$) of Ti6Al4V and Ti6Al4V-DopaMA. Error bars represent standard deviations, **** $p \leq 0.0001$. (c) XPS scans on the Ti6Al4V surfaces before and after DopaMA immobilization. (d) Dark field optical micrographs of PEGDMA-Oligo coating on Ti6Al4V-DopaMA vs Ti6Al4V IM pins (1 mm in diameter). Magnification: 50×.

h whereas significant colonization of *S. aureus* was detected on the PEGDMA-Oligo control hydrogel (Figure 2c, inset). The cleavage of the oligo linker by live *S. aureus* and the ability of released vancomycin to diffuse out of the hydrogel to exert antibiotic activities were further validated by the clear zone development around the PEGDMA-Oligo-Vanco hydrogels placed on an agar plate of the *S. aureus* culture. No clear zone was developed around the PEGDMA-Oligo control. These *in vitro* outcomes suggest that, when applied to the surface of implants, the PEGDMA-Oligo-Vanco hydrogel coating may also inhibit *S. aureus* surface attachment and colonization and suppress or even eradicate bacterial growth in its vicinity.

Hydrogel Coating of Ti6Al4V IM Pins. To evaluate the ability of PEGDMA-Oligo-Vanco hydrogel coating to prevent or mitigate periprosthetic infections *in vivo*, we applied the coating to the surface of Ti6Al4V IM pins emulating the metallic hardware used in orthopedic surgeries. To enhance the adhesion and stability of the hydrogel coating to the metallic substrate, the Ti6Al4V surface was first treated with dopamine methacrylate (DopaMA, Figure 3a). The catechol group from DopaMA is known for high affinity for surface oxides of Ti6Al4V[39] whereas the methacrylate is designed to covalently polymerize with the PEGDMA matrix during hydrogel coating application. Dip-coating the metallic substrate with DopaMA is expected to promote a more uniform and stable surface coating of the functionalized PEGDMA. The choice of the methacrylate surface group also makes it possible to covalently bond with poly(methyl methacrylate) (PMMA) bone cement if desired. Successful surface modification of Ti6Al4V plates (1 cm × cm) with DopaMA was confirmed by water contact angle measurements and X-ray photoelectron spectroscopy (XPS) analyses. A statistically significant increase in water contact angle (Figure 3b) was observed upon DopaMA surface coating, consistent with the increased surface hydrophobicity due to the bonding of the more hydrophilic catechol unit with surface oxides, exposing the hydrophobic methacrylate toward the air. Decreases in XPS signal intensities for Ti 2p and O 1s and an increase in intensity for C 1s were also observed upon DopaMA treatment, consistent with the surface coverage by the organic molecules (Figure 3c). Hydrogel precursors for PEGDMA-Oligo were then photopolymerized onto the DopaMA-coated Ti6Al4V surface. As shown by dark-field optical microscopy (Figure 3d), the DopaMA intermediate improved the uniformity of the PEGDMA-Oligo coating on the Ti6Al4V pins (0.5 mm in diameter; to be inserted into mouse femoral canal in subsequent *in vivo* studies). Vancomycin was then covalently attached to the hydrogel coating by EDC/NHS chemistry as described earlier. The antibacterial capability of PEGDMA-Oligo-Vanco-coated Ti6Al4V pins was validated by *in vitro* bacterial culture on LB agar plates (Figure S1).

***In Vivo* Antibacterial Activity of Ti6Al4V Pins Coated with PEGDMA-Oligo-Vanco Hydrogel.** A rodent femoral canal infection model[40,41] was used to investigate the antibacterial activity of the hydrogel-coated Ti6Al4V IM pins *in vivo*. A low dose (40 CFU) of bioluminescent Xen29 *S. aureus* was inoculated in the reamed femoral canal of skeletally mature CL57BL/6 mice (6−10 weeks old, males) before an unmodified Ti6Al4V pin, or a Ti6Al4V pin coated with PEGDMA-Oligo-Vanco or PEGDMA-Oligo hydrogel, was inserted (Figure S2). Our previous study showed that this low bacteria inoculation dose was sufficient in establishing infection in the mouse femoral canal.[21] The degree of infection was evaluated with longitudinal IVIS monitoring of the inoculated bacteria, quantification of total bacterial counts on retrieved pins, longitudinal microcomputed tomography (μCT) quantification of femoral bone changes, and histological staining of explanted femurs at the 21 day end point.

IVIS detected bioluminescence in the femurs receiving the IM pins coated with PEGDMA-Oligo control hydrogel at 2 days postoperation which was sustained over the course of 21 days (Figure 4a, bottom panel; Figure 4b, red bars). The

DOI: 10.1021/acscentsci.9b00870
ACS Cent. Sci. 2019, 5, 1929−1936

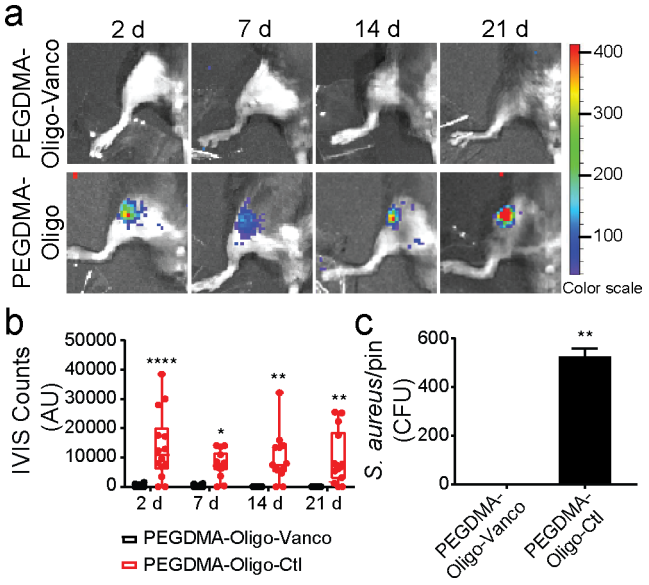

Figure 4. Complete eradication of *S. aureus* inoculated in the mouse femoral canal by PEGDMA-Oligo-Vanco coating. (a) IVIS images of mouse femurs injected with 40 CFU Xen-29 *S. aureus* and inserted with IM pins with PEGDMA-Oligo-Vanco or PEGDMA-Oligo coatings at 2, 7, 14, and 21 days. (b) Quantification of longitudinal bioluminescence signals of mouse femurs injected with 40 CFU Xen-29 *S. aureus* and inserted with the different hydrogel-coated pins at 2, 7, 14, and 21 days (n = 14). (c) *S. aureus* recovery from 21 day explanted pins (n = 11). Error bars represent standard deviations. * $p \leq 0.05$, ** $p \leq 0.01$, *** $p \leq 0.001$, **** $p \leq 0.0001$ (two-way ANOVA for part b; Student's t-test for part c).

longitudinal detection of bioluminescence in the no-vancomycin control coating group further validated the establishment of infection with the inoculation of 40 CFU Xen29 *S. aureus*. By stark contrast, no obvious bioluminescence was visualized from the femurs inserted with the IM pins coated with PEGDMA-Oligo-Vanco at any time point during the 21 day follow-up (Figure 4a, bottom panel), and the quantification of bioluminescent signals confirmed significant reduction in intensity by >95% at 2 days postoperation compared to the control groups (pins with PEGDMA-Oligo coating, Figure 4b, black bars; or unmodified pins, Figure S3), and complete disappearance after day 7 (Figure 4b, red bars). To confirm the elimination of bacterial burden by the PEGDMA-Oligo-Vanco coating *in vivo*, the IM pins were harvested on day 21 and thoroughly vortexed (5 min in LB media) before the suspensions were cultured on LB agar plates for bacterial counts. Consistent with the IVIS imaging data, no bacteria were recovered from the retrieved IM pins with PEGDMA-Oligo-Vanco coating, supporting complete eradication of periprosthetically bound bacteria while >500 CFU *S. aureus* were recovered from the retrieved IM pins with the PEGDMA-Oligo control coating (Figure 4c).

μCT imaging was carried out postoperation to confirm the proper positioning of inserted pins in all groups (Figure S4), and at the 3 week end point to determine the degree of infection within the femoral region of interest (ROI). Established local infections (osteomyelitis) could deteriorate the bone quality over time, causing decreases in bone volume fraction (BVF)[42] and bone mineral density (BMD),[43] and resulting in cortical thickening[44] in the affected area. Accordingly, these properties were quantified by end point μCT in both infected and uninfected femurs treated with IM pins with or without hydrogel coatings. 3D μCT axial slice images at the end point revealed osteolysis and an increase in cortical thickness (C. Th.), most clearly observed in the distal region of the infected femurs treated with unmodified pins (Figure S5a) or pins coated with PEGDMA-Oligo control hydrogel (Figure 5a). These changes were confirmed by the significant decreases in BVF and BMD accompanying the increase in C. Th. in the PEGDMA-Oligo + *S. aureus* group (Figure 5b) and the unmodified pin + *S. aureus* group (Figure S5b) compared to the uninfected groups or the infected group treated with pins coated with PEGDMA-Oligo-Vanco. The PEGDMA-Oligo-Vanco + *S. aureus* group showed no significant differences in BVF, BMD, or C. Th. when compared to uninfected control groups, suggesting that the coating effectively prevented the changes in bone architecture often seen in osteomyelitis.

Histological staining of explanted femurs was used to corroborate the morphological changes observed by μCT and to visualize any colonization or penetration of bacteria along the endosteal surface or within the canaliculi of the cortical bone. Hematoxylin and eosin (H&E) staining revealed normal cortical bone structure and bone marrow morphology in the PEGDMA-Oligo-Vanco + *S. aureus* group while pronounced cortical thickening was found in the PEGDMA-Oligo control + *S. aureus* (Figure 5c) and unmodified Ti6Al4V + *S. aureus* (Figure S6) groups, consistent with μCT findings. A highly cellularized bone marrow canal was also detected in the infected groups treated with unmodified pins (Figure S6, bottom row, *) or pins with the PEGDMA-Oligo control coating (Figure 5c, middle row, *), consistent with elevated cellular responses to an active local infection. No alkaline phosphatase (ALP, blue, osteoblasts) or tartrate-resistant acid phosphatase (TRAP, red, osteoclasts) activities, indicative of active bone remodeling, were found in the PEGDMA-Oligo-Vanco + *S. aureus* group (Figure 5c and Figure S6, top rows) or the uninfected groups (Figure S6, middle 2 rows). By contrast, infected femurs treated with unmodified pins (Figure S6, bottom row) or pins with the PEGDMA-Oligo control coating (Figure 5c, middle and bottom rows) exhibited coupled osteoblastic and osteoclastic activities within the cortical bone, consistent with the observed cortical thickening and enhanced remodeling within the cortices. Gram staining revealed colonized bacteria (blue) within the bone marrow canal of the PEGDMA-Oligo control + *S. aureus* (Figure 5c, middle and bottom rows) and unmodified pins + *S. aureus* groups (Figure S6, bottom row, inset) but not in the PEGDMA-Oligo-Vanco + *S. aureus* group (Figure 5c and Figure S6, top rows) or the control groups without *S. aureus* inoculation (Figure S6, 2 middle rows). No bacteria were detected in the cortical bone canaliculi by optical microscopy.

These μCT and histological findings strongly corroborated the bioluminescence data and end point bacterial counts on the retrieved pins to demonstrate the effectiveness of PEGDMA-Oligo-Vanco-coated Ti6Al4V pins in eradicating *S. aureus* within the marrow canal in a timely manner to prevent their colonization on the implant surface or invasion into the cortical bone. These outcomes represent a significant improvement over the short-range suppression of bacterial colonization on Ti6Al4V IM pins achieved by vancomycin covalently conjugated to either surface oxides[40] or to implant surface-grafted polymer brushes.[21] The on-demand release of vancomycin from the hydrogel coating enabled the bactericidal

DOI: 10.1021/acscentsci.9b00870
ACS Cent. Sci. 2019, 5, 1929−1936

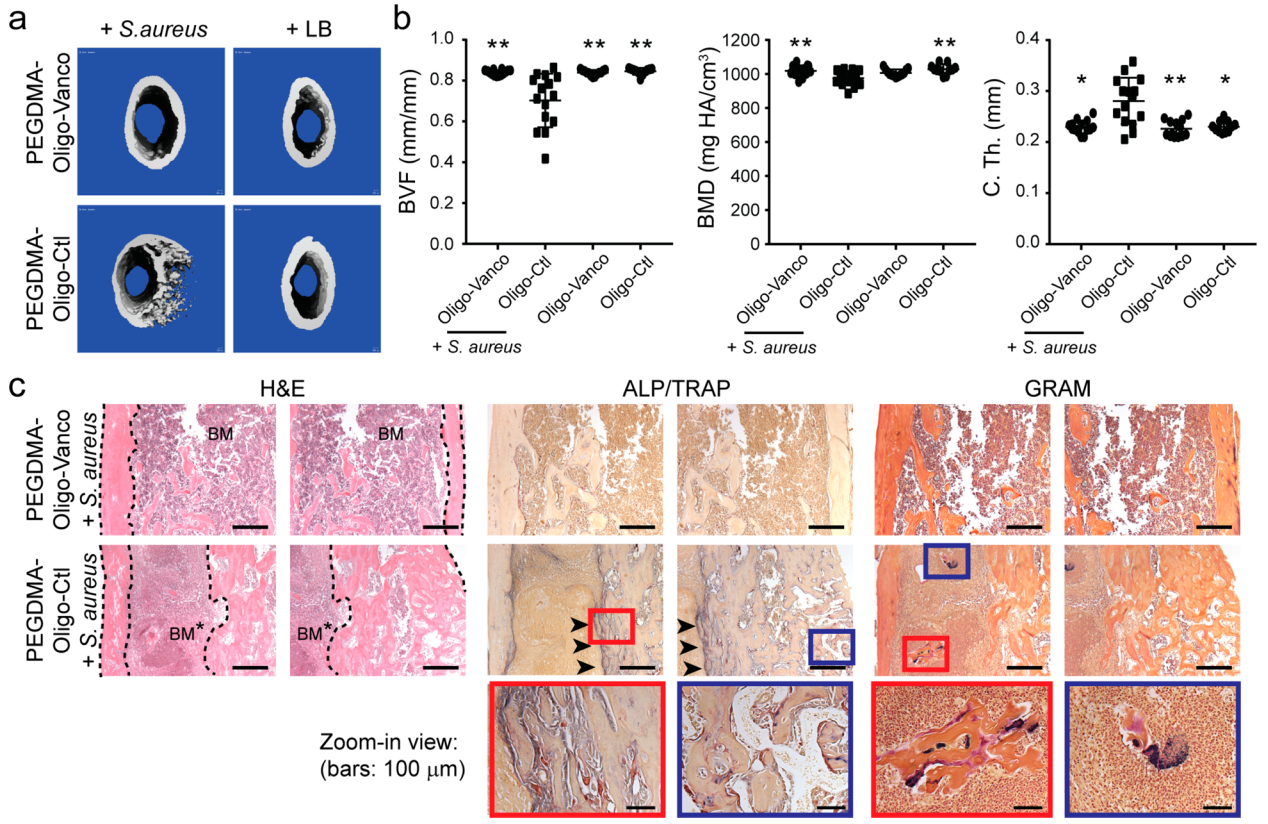

Figure 5. Prevention of the development of osteomyelitis in mouse femoral canal inoculated with *S. aureus* by PEGDMA-Oligo-Vanco coating. (a) 3D μCT axial images of the distal femoral region 21 days after the insertion of Ti6Al4V IM pins (pins excluded during contouring) with different hydrogel coatings, with or without the inoculation of 40-CFU Xen-29 *S. aureus*. (b) Quantification of femoral BVF, BMD, and C. Th. of infected and uninfected femurs 21 days after the insertion of Ti6Al4V IM pins with PEGDMA-Oligo-Vanco or PEGDMA-Oligo coatings. n = 11−14. Error bars represent standard deviations. * $p \leq 0.05$, ** $p \leq 0.01$ as compared to the PEGDMA-Oligo control coating + *S. aureus* group (one-way ANOVA). (c) H&E, ALP (blue)/TRAP (red), and Gram staining (bacteria stain blue) of explanted femurs in the infected group with PEGDMA-Oligo-Vanco coating or PEGDMA-Oligo control coating at 21 days postoperation. Dashed lines outline the cortical bone; BM = bone marrow; BM* = infected bone marrow; arrowheads indicate regions of enhanced ALP/TRAP activities; higher magnification views of the regions within the blue and red boxes are shown in the bottom row. Scale bars = 500 μm (top and middle rows) or 100 μm (bottom row).

properties of the freed vancomycin to be exerted in the broader periprosthetic tissue environment in a timely manner, clearing the bacteria before they had a chance to colonize on implant surfaces or invade the bone.

Scavenger organs harvested at 21 days postoperation revealed no difference among any of the groups treated with hydrogel-coated pins (both infected and uninfected) versus the healthy controls (Figure S7), supporting the safety of the coatings including the subsequently released vancomycin within the time frame examined. Such a safety profile is not surprising given that the polymethacrylate chemistry is employed in commercial bone cements, and the covalent vancomycin loading dose of 0.6 μg/mg PEGDMA applied to the Ti6Al4V IM pin was 200−400-fold lower than the common prophylactic antibiotics loading doses in commercial bone cement.[34−37]

Taken together, these *in vivo* results support outstanding bactericidal properties of the PEGDMA-Oligo-Vanco coating applied to Ti6Al4V pins to protect against *S. aureus* infections, eradicating the bacteria from both the implant surface and its periprosthetic bony tissue environment. The low dose of 40 CFU of *S. aureus* inoculated was sufficient to establish infection in the untreated groups and emulates a realistic clinical setting where, following standard debridement, gross infections prior to implantation are unlikely; it supports the validity of this model for examining the efficacy of prophylactic bactericidal coatings. By contrast, the literature shows that, in the absence of an MN-sensitive linker, antibiotics covalently attached to metallic implants can only reduce the bacterial colonization/biofilm formation on the implant surface[16,21,40] but are unable to release free-diffusing vancomycin to the broader periprosthetic tissue space to prevent the invasion, proliferation, and colonization to tissue and ultimately the development of chronic infections. A limitation of the current rodent study is the limited postoperation monitoring duration. To assess the long-term protection of this coating strategy against periprosthetic infections and its impact on implant osteointegration, a large animal study employing clinically used metallic implants, with/without porous surface topography, for up to 6 months would be desired. In addition, examining whether this coating strategy may be extended to bone cements and dental resins will also help determine the scope of its potential clinical translation.

CONCLUSIONS

In summary, the PEGDMA-Oligo-Vanco hydrogel coating applied to the surface of Ti6Al4V effectively prevented *S. aureus* colonization on the surface of the implants and eradicated local infection both *in vitro* and *in vivo*. The vancomycin was cleaved and released from the hydrogel

DOI: 10.1021/acscentsci.9b00870
ACS Cent. Sci. 2019, 5, 1929−1936

coating in the intramedullary space of mouse femurs inoculated with *S. aureus*, resulting in timely eradication of *S. aureus* from the implant surface and within the marrow cavity and preventing invasion of bacteria into cortical bone and the subsequent development of osteomyelitis. Conceptually, our findings support that early and timely bactericidal action by MN-triggered release of antibiotics is an effective prophylactic method to bypass the notoriously harder to treat periprosthetic biofilms and osteomyelitis.

From a translational perspective, the PEG-based polymethacrylate gelling mechanism was compatible with the solidification of bone cement and dental resin and, thus, may be applied as prophylactic standard care to prevent implant-associated biofilm formation and osteomyelitis. The DopaMA intermediate coating applied to the metallic implant surfaces ensures a stable and uniform hydrogel coating on the metallic implant surface. Finally, the low effective antibiotic tethering dose (e.g., more than 2 orders of magnitude reduction compared to prophylactic antibiotics physically blended with bone cement) and the MN-sensitive on-demand release mechanism improve both the efficacy (timely release) and safety of local antibiotics delivery.

■ ASSOCIATED CONTENT

Supporting Information

The Supporting Information is available free of charge at https://pubs.acs.org/doi/10.1021/acscentsci.9b00870.

Methods and supplementary figures showing LB agar plate containing PEGDMA-Oligo-Vanco and PEGDMA-Oligo-coated Ti6Al4V pins after 24 h of *S. aureus* culture, *in vivo* study design, longitudinal bioluminescence intensities of mouse femoral canals inserted with IM pins with or without PEGDMA-Oligo-Vanco coating, postoperation μCT axial images, 3D μCT axial images of the distal femoral region, histology staining of explanted femurs, and heart, lung, liver, spleen, pancreas, kidney, and rib retrieved from the mice receiving various IM pin treatments in uninfected vs infected femoral canals for 21 days (PDF)

■ AUTHOR INFORMATION

Corresponding Author

*E-mail: Jie.song@umassmed.edu.

ORCID

Ananta Ghimire: 0000-0003-0023-5355

Jie Song: 0000-0001-7554-5564

Notes

The authors declare no competing financial interest.

■ ACKNOWLEDGMENTS

The authors thank April Mason-Savas for histology support. XPS was performed at the Center for Nanoscale Systems (CNS) at Harvard University supported by the National Science Foundation award 1541959. This work was supported in part by a National Institute of Health grant (R01AR068418).

■ REFERENCES

(1) Wang, T.; Wang, C.; Zhou, S.; Xu, J.; Jiang, W.; Tan, L.; Fu, J. Nanovalves-Based Bacteria-Triggered, Self-Defensive Antibacterial Coating: Using Combination Therapy, Dual Stimuli-Responsiveness, and Multiple Release Modes for Treatment of Implant-Associated Infections. *Chem. Mater.* **2017**, *29* (19), 8325−8337.

(2) Zhao, L.; Chu, P. K.; Zhang, Y.; Wu, Z. Antibacterial coatings on titanium implants. *J. Biomed. Mater. Res., Part B* **2009**, *91* (1), 470−480.

(3) Campoccia, D.; Montanaro, L.; Arciola, C. R. The significance of infection related to orthopedic devices and issues of antibiotic resistance. *Biomaterials* **2006**, *27* (11), 2331−2339.

(4) Pichavant, L.; Carrie, H.; Nguyen, M. N.; Plawinski, L.; Durrieu, M. C.; Heroguez, V. Vancomycin Functionalized Nanoparticles for Bactericidal Biomaterial Surfaces. *Biomacromolecules* **2016**, *17* (4), 1339−1346.

(5) Cloutier, M.; Mantovani, D.; Rosei, F. Antibacterial Coatings: Challenges, Perspectives, and Opportunities. *Trends Biotechnol.* **2015**, *33* (11), 637−652.

(6) Yu, Q.; Wu, Z.; Chen, H. Dual-function antibacterial surfaces for biomedical applications. *Acta Biomater.* **2015**, *16*, 1−13.

(7) de Mesy Bentley, K. L.; Trombetta, R.; Nishitani, K.; Bello-Irizarry, S. N.; Ninomiya, M.; Zhang, L.; Chung, H. L.; McGrath, J. L.; Daiss, J. L.; Awad, H. A.; Kates, S. L.; Schwarz, E. M. Evidence of Staphylococcus aureus deformation, proliferation and migration in canaliculi of live cortical bone in murine models of osteomyelitis. *J. Bone Miner. Res.* **2017**, *32* (5), 985−990.

(8) Song, J.; Chen, Q.; Zhang, Y.; Diba, M.; Kolwijck, E.; Shao, J.; Jansen, J. A.; Yang, F.; Boccaccini, A. R.; Leeuwenburgh, S. C. Electrophoretic Deposition of Chitosan Coatings Modified with Gelatin Nanospheres To Tune the Release of Antibiotics. *ACS Appl. Mater. Interfaces* **2016**, *8* (22), 13785−13792.

(9) Bakhshandeh, S.; GorginKaraji, Z.; Lietaert, K.; Fluit, A. C.; Boel, C. H. E.; Vogely, H. C.; Vermonden, T.; Hennink, W. E.; Weinans, H.; Zadpoor, A. A.; Amin Yavari, S. Simultaneous Delivery of Multiple Antibacterial Agents from Additively Manufactured Porous Biomaterials to Fully Eradicate Planktonic and Adherent Staphylococcus aureus. *ACS Appl. Mater. Interfaces* **2017**, *9* (31), 25691−25699.

(10) Aldrich, A.; Kuss, M. A.; Duan, B.; Kielian, T. 3D Bioprinted Scaffolds Containing Viable Macrophages and Antibiotics Promote Clearance of Staphylococcus aureus Craniotomy-Associated Biofilm Infection. *ACS Appl. Mater. Interfaces* **2019**, *11* (13), 12298−12307.

(11) Zhuk, I.; Jariwala, F.; Attygalle, A. B.; Wu, Y.; Libera, M. R.; Sukhishvili, S. A. Self-Defensive Layer-by-Layer Films with Bacteria-Triggered Antibiotic Release. *ACS Nano* **2014**, *8* (8), 7733−7745.

(12) Anderson, E. M.; Noble, M. L.; Garty, S.; Ma, H.; Bryers, J. D.; Shen, T. T.; Ratner, B. D. Sustained release of antibiotic from poly(2-hydroxyethyl methacrylate) to prevent blinding infections after cataract surgery. *Biomaterials* **2009**, *30* (29), 5675−5681.

(13) Stewart, P. S.; William Costerton, J. Antibiotic resistance of bacteria in biofilms. *Lancet* **2001**, *358* (9276), 135−138.

(14) Wang, B.; Liu, H.; Sun, L.; Jin, Y.; Ding, X.; Li, L.; Ji, J.; Chen, H. Construction of High Drug Loading and Enzymatic Degradable Multilayer Films for Self-Defense Drug Release and Long Term Biofilm Inhibition. *Biomacromolecules* **2018**, *19* (1), 85−93.

(15) Taubes, G. The bacteria fight back. *Science* **2008**, *321*, 356−361.

(16) Chen, C. P.; Jing, R. Y.; Wickstrom, E. Covalent Attachment of Daptomycin to Ti6Al4V Alloy Surfaces by a Thioether Linkage to Inhibit Colonization by Staphylococcus aureus. *ACS Omega* **2017**, *2* (4), 1645−1652.

(17) Nie, B.; Long, T.; Ao, H.; Zhou, J.; Tang, T.; Yue, B. Covalent Immobilization of Enoxacin onto Titanium Implant Surfaces for Inhibiting Multiple Bacterial Species Infection and In Vivo Methicillin-Resistant Staphylococcus aureus Infection Prophylaxis. *Antimicrob. Agents Chemother.* **2017**, *61* (1), No. e01766-16.

(18) Jose, B.; Antoci, V.; Zeiger, A. R.; Wickstrom, E.; Hickok, N. J. Vancomycin Covalently Bonded to Titanium Beads Kills Staphylococcus aureus. *Chem. Biol.* **2005**, *12* (9), 1041−1048.

(19) Lawson, M. C.; Shoemaker, R.; Hoth, K. B.; Bowman, C. N.; Anseth, K. S. Polymerizable vancomycin derivatives for bactericidal biomaterial surface modification: structure-function evaluation. *Biomacromolecules* **2009**, *10* (8), 2221−2234.

DOI: 10.1021/acscentsci.9b00870
ACS Cent. Sci. 2019, 5, 1929−1936

(20) Walsh, C. Molecular mechanisms that confer antibacterial drug resistance. *Nature* **2000**, *406* (6797), 775−781.
(21) Zhang, B.; Braun, B. M.; Skelly, J. D.; Ayers, D. C.; Song, J. Significant Suppression of *Staphylococcus Aureus* Colonization on Intramedullary Ti6Al4V Implants Surface-Grafted with Vancomycin-Bearing Polymer Brushes. *ACS Appl. Mater. Interfaces* **2019**, *11* (32), 28641−28647.
(22) Gerits, E.; Kucharikova, S.; Van Dijck, P.; Erdtmann, M.; Krona, A.; Lovenklev, M.; Frohlich, M.; Dovgan, B.; Impellizzeri, F.; Braem, A.; Vleugels, J.; Robijns, S. C.; Steenackers, H. P.; Vanderleyden, J.; De Brucker, K.; Thevissen, K.; Cammue, B. P.; Fauvart, M.; Verstraeten, N.; Michiels, J. Antibacterial activity of a new broad-spectrum antibiotic covalently bound to titanium surfaces. *J. Orthop. Res.* **2016**, *34* (12), 2191−2198.
(23) Tang, F.; Li, L.; Chen, D. Mesoporous Silica Nanoparticles: Synthesis, Biocompatibility and Drug Delivery. *Adv. Mater.* **2012**, *24* (12), 1504−1534.
(24) Li, Z.; Yuan, D.; Jin, G.; Tan, B. H.; He, C. Facile Layer-by-Layer Self-Assembly toward Enantiomeric Poly(lactide) Stereocomplex Coated Magnetite Nanocarrier for Highly Tunable Drug Deliveries. *ACS Appl. Mater. Interfaces* **2016**, *8* (3), 1842−1853.
(25) Zhou, J.; Horev, B.; Hwang, G.; Klein, M. I.; Koo, H.; Benoit, D. S. Characterization and optimization of pH-responsive polymer nanoparticles for drug delivery to oral biofilms. *J. Mater. Chem. B* **2016**, *4* (18), 3075−3085.
(26) Yang, Z.; Mesiano, A. J.; Venkatasubramanian, S.; Gross, S. H.; Harris, J. M.; Russell, A. J. Activity and stability of enzymes incorporated into acrylic polymers. *J. Am. Chem. Soc.* **1995**, *117* (17), 4843−4850.
(27) Yan, M.; Ge, J.; Liu, Z.; Ouyang, P. Encapsulation of single enzyme in nanogel with enhanced biocatalytic activity and stability. *J. Am. Chem. Soc.* **2006**, *128* (34), 11008−11009.
(28) Hernandez, F. J.; Huang, L.; Olson, M. E.; Powers, K. M.; Hernandez, L. I.; Meyerholz, D. K.; Thedens, D. R.; Behlke, M. A.; Horswill, A. R.; McNamara, J. O., 2nd Noninvasive imaging of Staphylococcus aureus infections with a nuclease-activated probe. *Nat. Med.* **2014**, *20* (3), 301−306.
(29) Hernandez, F. J.; Hernandez, L. I.; Kavruk, M.; Arica, Y. M.; Bayramoglu, G.; Borsa, B. A.; Oktem, H. A.; Schafer, T.; Ozalp, V. C. NanoKeepers: stimuli responsive nanocapsules for programmed specific targeting and drug delivery. *Chem. Commun. (Cambridge, U. K.)* **2014**, *50* (67), 9489−9492.
(30) Borsa, B. A.; Tuna, B. G.; Hernandez, F. J.; Hernandez, L. I.; Bayramoglu, G.; Arica, M. Y.; Ozalp, V. C. Staphylococcus aureus detection in blood samples by silica nanoparticle-oligonucleotides conjugates. *Biosens. Bioelectron.* **2016**, *86*, 27−32.
(31) Grundmann, H.; Aires-de-Sousa, M.; Boyce, J.; Tiemersma, E. Emergence and resurgence of meticillin-resistant Staphylococcus aureus as a public-health threat. *Lancet* **2006**, *368* (9538), 874−885.
(32) Kahne, D.; Leimkuhler, C.; Lu, W.; Walsh, C. Glycopeptide and lipoglycopeptide antibiotics. *Chem. Rev.* **2005**, *105* (2), 425−448.
(33) Lawson, M. C.; Shoemaker, R.; Hoth, K. B.; Bowman, C. N.; Anseth, K. S. Polymerizable Vancomycin Derivatives for Bactericidal Biomaterial Surface Modification: Structure-Function Evaluation. *Biomacromolecules* **2009**, *10* (8), 2221−2234.
(34) Bistolfi, A.; Massazza, G.; Verné, E.; Massè, A.; Deledda, D.; Ferraris, S.; Miola, M.; Galetto, F.; Crova, M. Antibiotic-Loaded Cement in Orthopedic Surgery: A Review. *ISRN Orthop* **2011**, *2011*, 1.
(35) Neut, D.; de Groot, E. P.; Kowalski, R. S.; van Horn, J. R.; van der Mei, H. C.; Busscher, H. J. Gentamicin-loaded bone cement with clindamycin or fusidic acid added: biofilm formation and antibiotic release. *J. Biomed. Mater. Res., Part A* **2005**, *73* (2), 165−170.
(36) Meyer, J.; Piller, G.; Spiegel, C. A.; Hetzel, S.; Squire, M. Vacuum-mixing significantly changes antibiotic elution characteristics of commercially available antibiotic-impregnated bone cements. *J. Bone Joint Surg. Am.* **2011**, *93* (22), 2049−2056.
(37) Jiranek, W. A.; Hanssen, A. D.; Greenwald, A. S. Antibiotic-loaded bone cement for infection prophylaxis in total joint replacement. *J. Bone Joint Surg. Am.* **2006**, *88* (11), 2487−2500.
(38) Francis, K. P.; Joh, D.; Bellinger-Kawahara, C.; Hawkinson, M. J.; Purchio, T. F.; Contag, P. R. Monitoring bioluminescent Staphylococcus aureus infections in living mice using a novel luxABCDE construct. *Infect. Immun.* **2000**, *68* (6), 3594−3600.
(39) Lyu, Q.; Hsueh, N.; Chai, C. L. L. The Chemistry of Bioinspired Catechol(amine)-Based Coatings. *ACS Biomater. Sci. Eng.* **2019**, *5* (6), 2708−2724.
(40) Antoci, V., Jr.; Adams, C. S.; Hickok, N. J.; Shapiro, I. M.; Parvizi, J. Vancomycin bound to Ti rods reduces periprosthetic infection: preliminary study. *Clin. Orthop. Relat. Res.* **2007**, *461*, 88−95.
(41) Adams, C. S.; Antoci, V., Jr.; Harrison, G.; Patal, P.; Freeman, T. A.; Shapiro, I. M.; Parvizi, J.; Hickok, N. J.; Radin, S.; Ducheyne, P. Controlled release of vancomycin from thin sol-gel films on implant surfaces successfully controls osteomyelitis. *J. Orthop. Res.* **2009**, *27* (6), 701−709.
(42) Stadelmann, V. A.; Potapova, I.; Camenisch, K.; Nehrbass, D.; Richards, R. G.; Moriarty, T. F. In Vivo MicroCT Monitoring of Osteomyelitis in a Rat Model. *BioMed Res. Int.* **2015**, *2015*, 587857.
(43) Niska, J. A.; Meganck, J. A.; Pribaz, J. R.; Shahbazian, J. H.; Lim, E.; Zhang, N.; Rice, B. W.; Akin, A.; Ramos, R. I.; Bernthal, N. M.; Francis, K. P.; Miller, L. S. Monitoring bacterial burden, inflammation and bone damage longitudinally using optical and muCT imaging in an orthopaedic implant infection in mice. *PLoS One* **2012**, *7* (10), No. e47397.
(44) Odekerken, J. C.; Walenkamp, G. H.; Brans, B. T.; Welting, T. J.; Arts, J. J. The longitudinal assessment of osteomyelitis development by molecular imaging in a rabbit model. *BioMed Res. Int.* **2014**, *2014*, 424652.

DOI: 10.1021/acscentsci.9b00870
ACS Cent. Sci. 2019, 5, 1929−1936